Through-Thickness Permeability of Woven Fabric Under Low Air Pressure

XIAO Xueliang[1], QIAN Kun[1*], LONG Andrew[2]

[1] School of Textiles and Clothing，Jiangnan University

[2] School of Mechanical, Materials and Manufacturing Engineering, Nottingham University

*肖學良 Email: xiao_xueliang@jiangnan.edu.cn

Abstract

Through-thickness permeability (TTP) is one primary property of technical textiles used in air-related applications, such as filtration and protection. The TTP depends on the textile geometrical factors and usually varies according to the test conditions. In this article, the effect of low air-pressure compression (LPC) on TTP of woven fabric was investigated. Nine woven fabrics were measured for the relationships of LPC and thickness, LPC and fabric in-plane dimensions, air pressure drop (APD) and air velocity, as well as LPC and fabric TTP. A dramatic decrease of woven fabric thickness was found below the APD value of 200 Pa and less decreased thickness was observed with a continue increase of APD. The variation of fabric in-planar dimensions was found neglectable during LPC. The plot relationship of the APD and measured air velocity was presented in linearity for most fabric samples. The fabric TTP showed a linear proportion to the fabric thickness, indicating the fabric to be more permeable with the increase of thickness. Sensitivity study showed an evident difference between using fabric constant and decreased (LPC) thickness in calculating TTP, disclosing the importance of compression in fabric TTP evaluation.

Keywords: Air Permeability, Compression, Through-Thickness Direction, Woven Fabric

Introduction

Permeability measures the ability of a porous medium to transmit fluids. It depends on the porous geometrical structure [1]. As known, a plain or twill woven fabric consists of two sets of perpendicular interlaced yarns, namely warps and wefts, thus, its air permeability (K_f) is determined by the geometry and dimension of its intergaps (pores between warps and wefts) and intrapores (pores inside yarns). However, owing to the low stiffness [2], fabric is easily compressed under a through-thickness air pressure [3], giving rise to the yarn crossover tighter and the yarn path flatter. The yarn cross-section is thereafter in a more flat-oval/flat-elliptical shape [4]. This is often encountered during the fabric air permeability test where woven fabric is normally compressed by the applied air pressure drop (ΔP). Therefore, it is attractive to study the 'real' K_f value of a woven fabric considering the fabric compression. Moreover, when woven fabric is applied to polymer composite or airbag, a transient compression usually takes place in composites processing or airbag inflation which may cause a dynamic K_f value and influence the manufacture or protective efficiencies. Hence, the mechanism of dynamic K_f due to the transient ΔP is desired for optimizing the design of protective textiles and composites processing. In this article, K_f of two-dimensional (2D) woven fabric under transient compression is studied, as a comparison to the conventional air permeability test with suggested constant ΔP values of 50 Pa in standard BS-EN-ISO-9237: 1995 [5] and 125 Pa in standard ASTM-D737-R2012 [6].

Compression of a 2D-woven fabric has been extensively investigated experimentally and analytically [7-10]. The pressure-thickness curve of a woven fabric under low load is usually obtained according to the test standard of Kawabata Evaluation System (KES-Compression).

As shown one case of the curve in Fig.1, the first part is non-linear showing a dramatic decrease of thickness as increase of the load. This region reveals a very low modulus of woven fabric, and then followed by a rapid increase of load with lower decrease of fabric thickness. The final stage of the curve shows close to a straight line whose slope is extremely low, indicating that the fabric is hard to compress when the pressure is greater than a critical value.
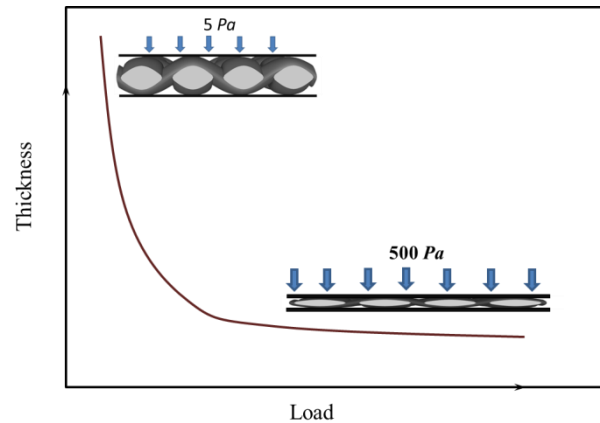
Figure 1 Relationship of the fabric thickness with the compression load

There are two fabric compression mechanisms to interpret the behavior [9]: the yarn cross-sectional compaction, and the yarn bending accompanied with the yarn path flattening. It was reported [9] that the woven fabric compression is very sensitive to the initial yarn fibre volume fraction (V_f) which affects the behavior in two ways. The first way is that the yarn itself becomes harder to compress while the second way is manifested through the more difficulty in macro-bending deformation of yarn as V_f increases. Physically, a smaller V_f value indicates more room for the yarn to be compacted, and hence it is easier for the woven fabric to be compacted, and vice versa. However, KES test for the fabric compression is based on a small circular plate which performs on the yarn crossover first, followed towards the inclined part of yarns. In this article, test of uniform air pressure on fabric anywhere and corresponding pressure-thickness curve in compression are required, which can mimic the effect of air pressure on the fabric K_f measurement.

The K_f value of a 2D-woven fabric is determined by the fabric internal geometry, especially the shape of air channels formed by intra-yarns and inter-yarns. Early researchers focused on the yarn (fibre bundles) permeability (K_y) [11-16] based on the ideal and stochastic filaments arrays, which was proven to be two or three times of magnitude order smaller than the K_f value of woven fabric which has clear gaps between warp and weft yarns, since air always tries its easiest way to flow through. Later, researchers paid much attention to the gap geometry using cylinder model [17,18], hydraulic diameter model [19], parabolic curve model [20], etc. These models show the gap permeability (K_g) usually much larger than the K_f value which contains fabric porosity ($\emptyset$). As a fact, the ratio of gap area to fabric area, i.e. $\emptyset$, affects the K_f value significantly [21]. This is due to the fact that friction among the internal air, air and fibre interface becomes less than the air flow through pure yarns without interlaced gaps. Experimental data have confirmed the small percentage of K_y to K_f when $\emptyset$ is larger than a critical value (1%) [22,28]. Yarns are then normally regarded as solid state ($K_y \approx 0$), and K_f mainly consists of $\emptyset$ and K_g.

The K_f test standards are usually under hypothesis of constant fabric architecture [5,6]. However, for a set of increasing air pressures up to hundreds of Pascals, it is found an evident nonlinear decrease of thickness as shown the case in Fig.1. This may lead to K_f a dynamic value based on Darcy's law [23]:

$$\Delta P = \frac{\mu L V}{K_f} \qquad (1)$$

where μ is the fluid viscosity which is normally regarded as a constant value, V is the flow velocity, L is the flow length, i.e. fabric thickness. Without out-of-plane fabric deflection, this article investigates the effect of dynamic fabric thickness under low air pressures on the transient fabric permeability, analytically and experimentally.

Analysis of K_f of woven fabric under low air pressures

When an air pressure drop is performed on the two sides of a woven fabric, air flow occurs through the porous structural fabric. It is noted that the most air flow streamlines take place at the gaps between warps and wefts due to the nature that air always finds its easiest way to flow. This air flow behavior can be simulated from a real weave architecture (Fig.2a), as shown the air streamlines in a unit cell of woven fabric in Fig.2d based on the TexGen (Fig.2b and c) [24] and CFD [25] simulations.
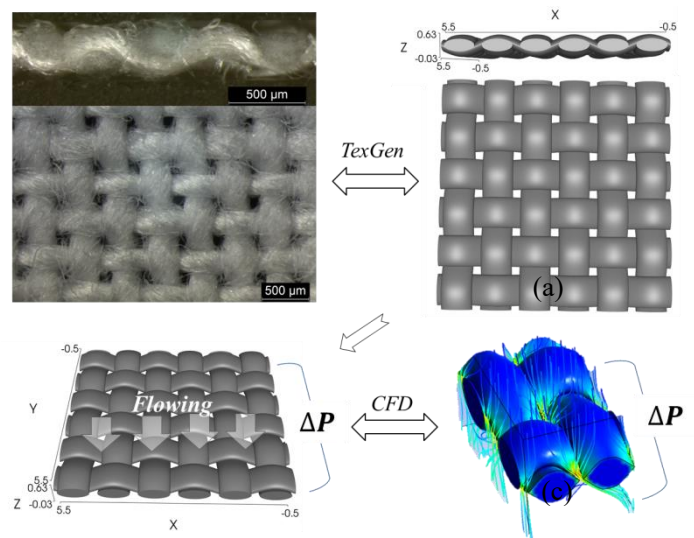
Figure 2 Illustrations of (a) a real and (b) a simulated woven fabric architecture, and laminar flow through (c) a woven fabric and (d) its unit-cell through CFD simulation

As known, the regular structure of woven fabric gives rise to arrays of air flow channels, which are in theory identical and repetitive. The geometry of each individual air flow channel is mainly determined by weave porosity, yarn cross- section and fabric thickness. The K_f of woven fabric is governed by these geometric parameters. In this article, we simplify different weave patterns (plain, twill and satin as shown in Fig.3a) into the same format of a converging-diverging air flow channel (Fig.3b) according to the hydraulic-diameter conversion theory [19,26], i.e. Eqs.2 and 3.

$$R = \frac{(S_j - D_j)(S_w - D_w)}{2(S_j - D_j + S_w - D_w)} \qquad (2)$$

$$a = \frac{S_j S_w}{2(S_j + S_w)} - R \qquad (3)$$

where R is the radius of the narrowest cross-section and a is the distance from the narrowest channel surface to the boundary of unit-cell as shown in Fig.3c, j and w represent warp and weft direction, respectively. A (x, y) coordinate is set for the hydraulic converging-diverging air flow channel. Figure.3a shows three rectangular unit-cells of weave patterns as

air flow channels, which have the dimensions of yarn spacing $(S_j, S_w,)$, yarn width $(D_j, D_w,)$ and fabric thickness (L).

We assume that (1) air flow is always creeping or laminar under the test pressure drop, (2) K_y equals to zero since the majority of air flow passes the gaps between the interlaced yarns, (3) slippage within yarns and fabric in planar dimension under LPC can be neglected.
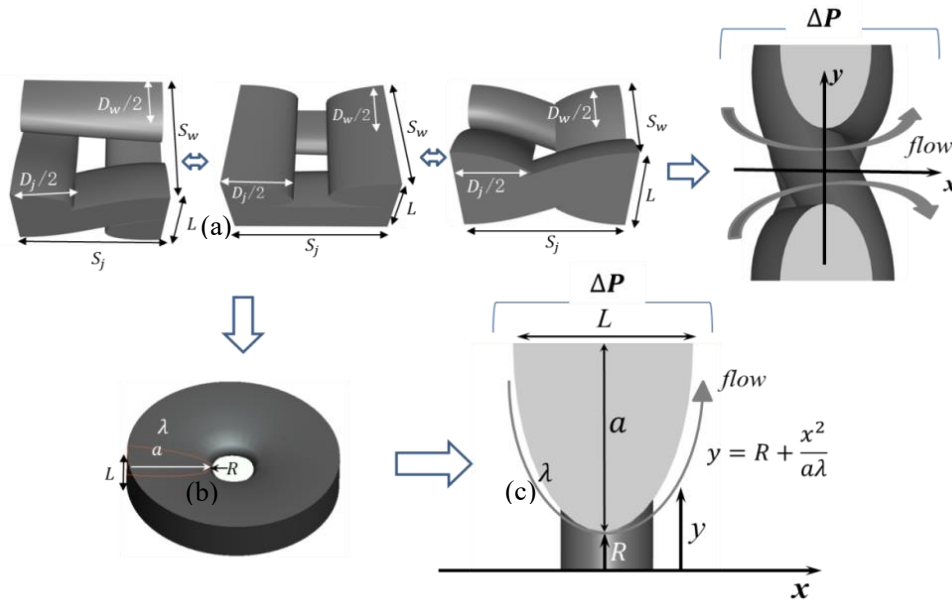
Figure 3 (a) Unit-cells of three rectangular gaps between yarns, (b) a simplified air flow channel, and (c) air flow channel curve fitted using a parabola

A parabolic equation is proposed to describe the air flow streamline along the smooth wall of the simplified air flow channel as shown in Fig.3b:

$$y = R + \frac{x^2}{\lambda a} \qquad (4)$$

where λ is a parameter that determines the curved flow-channel geometry, which can be tested experimentally by a microscope using fabric cross-section cured by epoxy resin. λ is an independent parameter from S_j, S_w, D_j, D_w and L, and a smaller λ value means a sharper boundary of yarn cross-section. The classical fluid dynamics discusses a situation of creeping or laminar flow through a circular tube, namely the Hagen-Poiseuille equation [27]:

$$Q = \frac{\pi y^4}{8\mu} \frac{\Delta P}{L} \qquad (5)$$

where Q is the volumetric flow rate, y is the radius of the tube and $\Delta P / L$ is the pressure gradient along the tube. By substituting Eq.4 into Eq.5 represents that the shape of air flow streamline has a change from straight into parabolic according to the equivalent flow shear distribution on the basis of the lubrication theory [11].

$$\int_{P_1}^{P_2} dP = \int_{-\frac{L}{2}}^{\frac{L}{2}} \frac{8\mu Q}{\pi \left(R + \frac{x^2}{\lambda a}\right)^4} dx \qquad (6)$$

After integration of Eq.6 following with a simplification process [19], an expression is obtained for the relationship of Q and ΔP, V and ΔP:

$$Q = \frac{2\Delta P}{5\mu} \frac{R^4}{\sqrt{\lambda aR}} \qquad (7)$$

$$V = \frac{2\Delta P}{5\pi\mu} \frac{R^4}{(R+a)^2\sqrt{\lambda aR}} \qquad (8)$$

Equation 8 shows a linear proportion relationship of air ΔP and V. Based on Eq.1, the semi-static K_g and K_f under a certain ΔP value are obtained as follows:

$$K_g = \frac{2R^2}{5\pi} \frac{L}{\sqrt{\lambda aR}} \qquad (9)$$

$$K_f = \frac{2R^4}{5\pi(R+a)^2} \frac{L}{\sqrt{\lambda aR}} \qquad (10)$$

From Eqs. 9 and 10, it is noted that K_f equals to K_g multiplied by fabric $\emptyset$ which is $R^2/(R + a)^2$. Eq.10 is obtained by assuming zero of K_y. When $R = 0$, Eq.10 does not apply to fabric K_f prediction, where K_f actually equals to its K_y value.

On the other hand, L in Eqs.9 and 10 are never constant when air ΔP varies, indicating K_f may be a function of LPC if considering the change of L. From Fig.1 and experimental data, it was given an empirical equation for L during LPC [7]:

$$\Delta P = \frac{\epsilon}{(L^o - L')^3} \qquad (11)$$

where L^o is the L without compression, L' is the L under ΔP compaction, ϵ is a fitting factor depending on the fibre materials and weave styles. From Eqs.10 and 11, it is notable that K_f is a static value for a specific ΔP value, however, for the ΔP values, K_f may exhibit dynamic due to the change of L.

Experimental materials and methodology

Nine woven fabrics were prepared for K_f investigation. The fabric geometrical dimensions were measured three times for each average value using a Leica microscope, and the specifications are listed in Table 1. Yarns in plain woven fabrics U_{1-3} are made of pure cotton staple fibres under 'Z' spinning style from a ring spun system with a set twist value 858 t/m, and the number of warps and wefts per centimetre (Nj/cm,

Nw/cm) are 21.3 and 24.4 for fabric U_1, 42.6 and 27.4 for fabric U_2, 51.3 and 27.6 for fabric U_3, respectively. Plain woven fabric A_1 and A_3 are tight structural fabrics both made of pure nylon filaments without any twist. The Nj/cm and Nw/cm values are 22.2 and 19.8 for fabric A_1 and 28.1 and 27 for fabric A_3. Twill woven fabrics C_{7-10} are made of blended staple fibres under "Z" spinning style. The yarns are all made with twist of 812 t/m, and the fabrics C_{7-8} are in 2/1 twill pattern and C_{9-10} are in 2/2 twill pattern. The Nj/cm values for fabrics C_{7-10} are 29.4, 29.4, 28.1 and 29.2, respectively while the corresponding Nw/cm values are 22.2, 23.3, 19.2 and 22.4, respectively. Post treatment and finishing procedure of fabrics are also listed in Table 1 since we believe finishing techniques may have appreciable effects upon air permeability by causing changes of air flow channels through a fabric.

Three devices were employed, i.e. a Leica optical microscope (M165C), a self-built dynamic thickness tester and a FX 3300 fabric air permeability tester, for measuring the dimensions of fabric geometrical parameters, the thickness under LPC and the relationship of air pressure drop and air velocity, respectively. Figure 4a illustrates our self-built dynamic thickness tester which can measure the transient fabric thickness under corresponding LPC. A stress-free flat fabric (b') is clamped by two plates (e') with six bolts (g') on a metal mesh (a') with high stiffness. The metal mesh ($\emptyset = 0.25$) simulates a fabric platform which has negligible resistance to air flow and negligible out-of-plane deflection during the exerted ΔPs. The edge of a' and b' is sealed by a compressed rubber ring (o') in plates. The test diameter of the fabric in this device is 41 mm. The air in the container (f') is pumped by a vacuum pump (d'), causing a LPC between the two sides of clamped fabric. There is a valve (v') that can control the LPC level. A vacuum pressure gauge (c') gives the LPC reading for the different pressures of the two sides of the clamped fabric. A ruler is placed on the top plate across a diameter parallel to the fabric, and a vernier

calliper (0.01 *mm*) is perpendicularly placed on the ruler and movable to determine the deduction of fabric thickness. Each fabric thickness under a certain LPC was repeated five times with a fresh sample. Figure.4b shows that the variation of in-plane dimensions of woven fabric can be observed by a microscope (Leica, M165C) on the LPC test device. The microscope can give a maximum magnification of 7.5 which can observe the fabric repeat unit cell clearly.

Table 1 Geometrical fabric parameters for nine woven fabrics (mean value)

Fabric	Composition*// Structure	λ	Yarn spacing** (*mm*)		Yarn width** (*mm*)	
			warp	weft	warp	weft
U_1	100% cotton yarns (31.2 *tex*)//plain	6.284	0.470	0.410	0.405	0.279
U_2	100% mercerised cotton yarns (13.4 *tex*)//plain	4.755	0.235	0.365	0.195	0.255
U_3	100% mercerised, bleached cotton poplin yarns (13.4 *tex*)//plain	7.566	0.295	0.362	0.193	0.200
A_1	100% nylon, airbag fabric yarns (50.6 *tex*)// plain	-	0.450	0.506	0.513	0.453
A_3	100% nylon, airbag fabric yarns (24.7 *tex*)// plain	0.580	0.356	0.370	0.350	0.300
C_7	67% PET/ 33% cotton, desized, scoured, bleached and mercerised yarns (41.2 *tex*)//2/1twill	6.920	0.340	0.450	0.300	0.400
C_8	67% PET/ 33% cotton, finished yarns (43.5 *tex*)//2/1twill	8.253	0.340	0.430	0.300	0.350
C_9	60% cotton/ 40% PET, desized, scoured, bleached and mercerised yarns (53.4 *tex*)//2/2twill	1.274	0.356	0.520	0.332	0.450
C_{10}	60% cotton/ 40% PET, finished yarns (60.9 *tex*)//2/2 twill	4.100	0.342	0.446	0.313	0.380

*Note: Warp and weft yarns in each fabric are identical.
**Definition: Yarn spacing- the distance between two neighboring parallel yarn centerlines; Yarn width- the distance of a yarn cross section in planar.
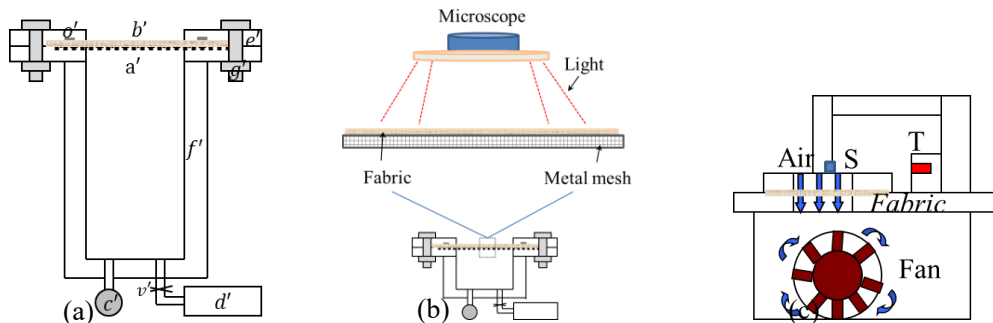
Figure 4 Measurement principle of (a) a fabric LPC self-built thickness tester, (b) the fabric LPC observation by a Leica microscope, (c) a FX-3300 air permeability tester

Figure.4c illustrates the work principle of an air permeability tester (FX-3300): a woven fabric is clamped with the test area 10 *cm²*. Such test area gives around 3.5 *cm* diameter of a fabric under LPC (hundreds of Pascals). The fabric out-of-plane deflection is ignored due to the fabric high in-plane strain energy [28]. *T* is a transducer that can control the LPC levels between the clamped fabric surfaces and *S* is a sensor that can determine the volumetric flow rate (*Q*, *m³/s*) which divided by the test area gives the superficial velocity (*V*, *m/s*) of the air flow. A number of LPCs was implemented, i.e. 25 Pa, 50 Pa, 75 Pa, 100 Pa, 250 Pa, 500 Pa, 750 Pa, 1000 Pa and 1500 Pa, etc. Using the measured parameters of *V*, ΔP and *L*, the measured K_f is calculated according to Eq.1 for each applied ΔP. Each test was repeated three times with a fresh sample.

Results and discussions

Fabric dimensions under LPC
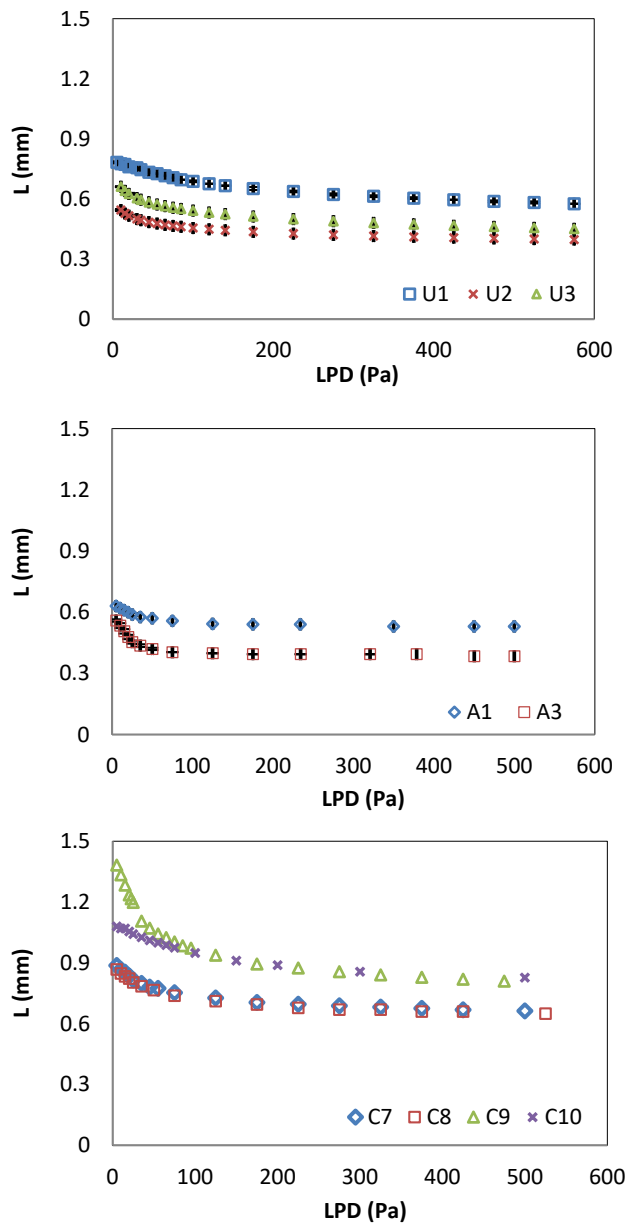
Figure 5 Variation of fabric thickness over low pressure drops (LPD) for three groups of woven fabrics: (a) U*x*, (b) A*x* and (c) C*x*

The fabric thickness (L) under LPC obtained from the dynamic thickness tester was sorted into thickness-pressure curves, as shown in Fig.5. It is observed that the most sensitive compaction of all fabrics is below 200 Pa owing to the low initial V_f value at yarn float and crossover. The measured fabric thickness-pressure curves indicate that the fabric compaction under air ΔP is consistent with the classical plate fabric compression where the easiest compaction occurs at the initial loading, followed with less compression for the same increase of pressure [29-31]. Figure 5 compares the L reduction of three

fabric groups under LPC, and finds that fabrics U_3, A_3 and C_9 are compacted with the largest reduction of L in each group. This may be ascribed to the fact that these fabrics have relative lower V_f and larger $\emptyset$ values as results of easier compaction at yarn crossovers and bending at gaps between interlaced yarns. Owing to the high modulus of nylon filaments and the overlapping yarns, fabric A_1 shows the smallest compaction at the test LPC region. It is also notable that fabrics C_7 and C_8 have the similar compaction behaviour for their similar compositions and architectures with slight different post treatments.
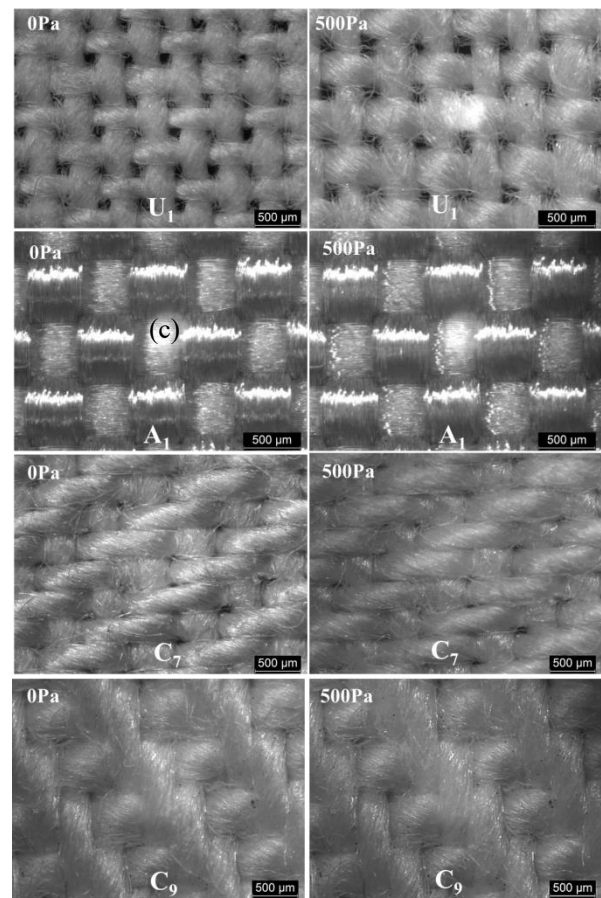
Figure 6 Top views of woven fabrics (a) U₁, (b) A₁, (c) C₇ and (d) C₉ without and with 500 Pa of air compression

Figure 6 shows the top views of four typical fabrics ((a) plain woven fabric U_1 with clear gaps and (b) plain woven fabric A_1 with overlapping-yarns, twill woven fabrics of (c) 1/2 C_7 and (d) 2/2 C_9) at free state and 500 Pa of compaction. The yarns in fabrics U_1, C_7 and C_9 display twisted texture for tightening the staple fibres, which leads to K_y much smaller than K_g,

suggesting the necessity of ignorance of K_y in K_f prediction. Fabric A_1 shows a tight structure of overlapping yarns ($\emptyset=0$) consisting of long parallel filaments without twist, implying that space among inter-filaments dominates K_f of fabric A_1. The comparison of fabric under free-state and LPC in Fig.6 indicates that the change of in-planar gap dimensions can be ignored below the air ΔP of 500 Pa for less than 0.1% of in-planar dimensions variation.
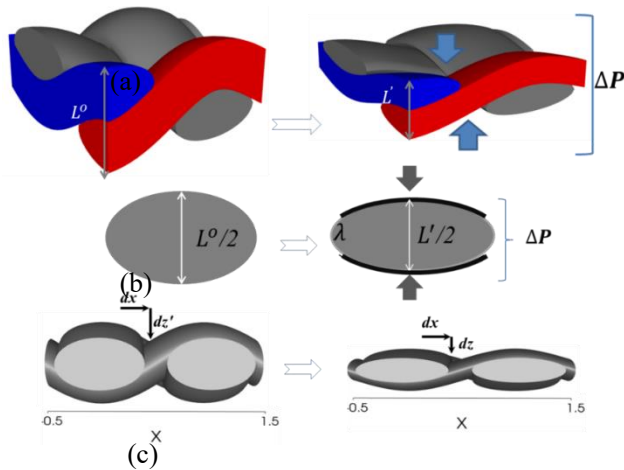
Figure 7 Schematic illustrations of (a) fabric compression, (b) yarn cross-section under a pressure drop, and (c) hydraulic resistance of long and short air flow channels

Up to this LPC, fabric deformation is mainly attributed to the increased V_f value and reflected through the reduced space among intra-filaments and the decreased height of yarn crossover and cross-section. This is shown by the schematic diagram of Fig.7 which illustrates the deformation of a woven fabric under a small ΔP value. The oval/elliptical yarn cross-section is assumed with the same λ value after compression for only the reduced yarn height. Different from airbag fabrics with out-of-plane deflection under an inflation impact of ΔP value between 0.1 and 10 million Pascals, the small ΔP values can only cause the yarn V_f value increased due to the decreased L value. On the basis of the measured pressure-thickness curves, constant in-planar geometrical dimensions and Eqs.1, 10 and 11, a relationship of K_f and L should be studied during LPC experimentally for the nine fabrics.

Relationship of K_f and LPC

(a)

(b)
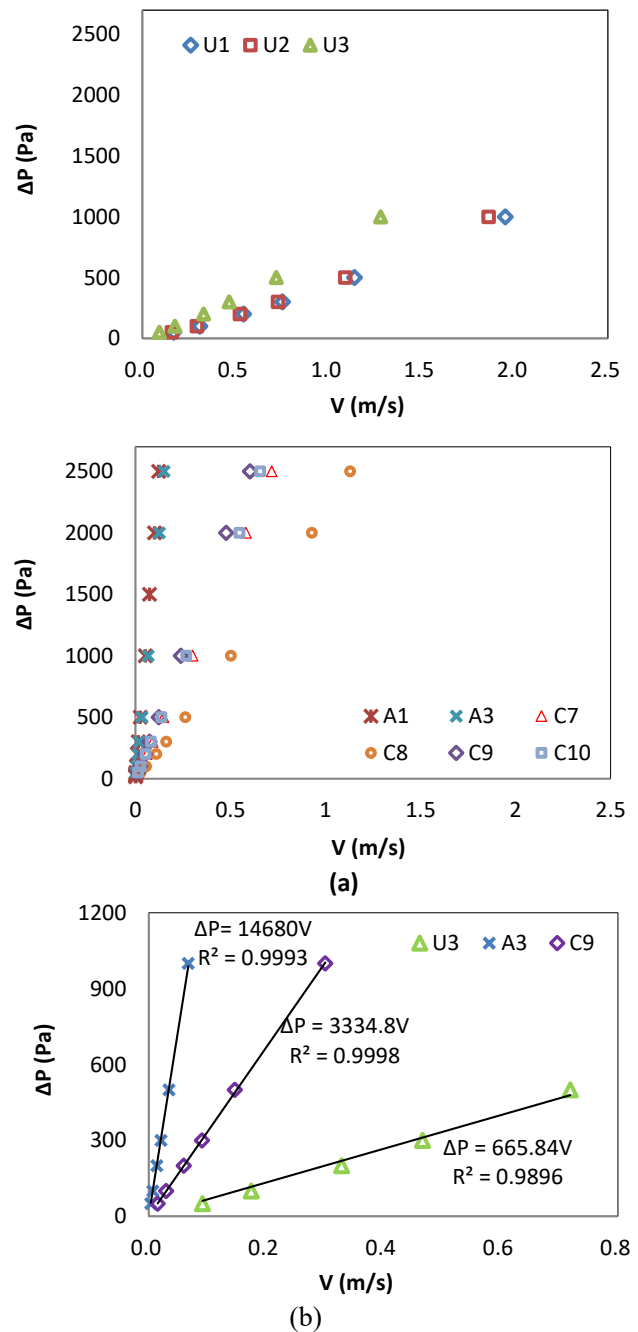
Figure 8 (a) Experimental data of air pressure drop and air velocity for nine fabrics; (b) curve fitting for the relationship of three typical fabrics

Fabrics are compacted under ΔP, and Fig.8a shows the tested relationship of a set of ΔPs and corresponding air velocities (V s) for the nine compacted woven fabrics. It is noted that most relationships display linearity in the test range while slight nonlinear curves are presented by fabrics U_{1-3}, however, the non-linearity of curves shows evident local linearity below the ΔP value of 200 Pa. The

experimental compression in Fig.5 showed remarkable decreased L of fabrics U_3, A_3 and C_9 under LPC. However, the fitting equations between ΔP and V values show strong linearity for the fabrics (U_3, A_3 & C_9) according to Eq.1 with the fitted R^2 values very close to 1, as shown in Fig.8b. Thus, for most fabrics, the values of $\Delta P/V$ (slope of the fitting line for experimental data) are constant. Assuming μ is a constant value in the test ΔP range, we have a conversion of Eq.1, which is $\Delta P/V = \mu \cdot L/K_f$. Based on this expression, the dynamic K_f value of a fabric under LPC depends on the variation of L which is consistent with the linearity ($L/K_f \propto$ in-planar geometrical dimensions) of Eq.10.

On the basis of the tested Ls under LPC (Fig.5), a set of experimental K_f values of nine fabrics can be calculated by Eq.1 using the applied ΔPs and the measured Vs. Herein, K_f means the ability of a woven fabric to transmit air, a larger K_f value indicates the air to be easier to transverse a fabric. Figure 9 shows the scattered K_f values of the nine fabrics tested in the same LPC region. For each fabric, the tested K_f values can be fitted in linearity. This is consistent with the analytical prediction in each corresponding line, which is based on Eq.10 assuming constants of other geometrical parameters. The close relationship of the prediction lines with the experimental dots in Fig.9 indicates the good accuracy of Eqs.2-4, 10 & 11 in predicting K_f of woven fabric under LPC. Due to the structure of overlapping-yarns, the K_f prediction of fabric A_1 was based on the Gebart model without K_g [11, 22].
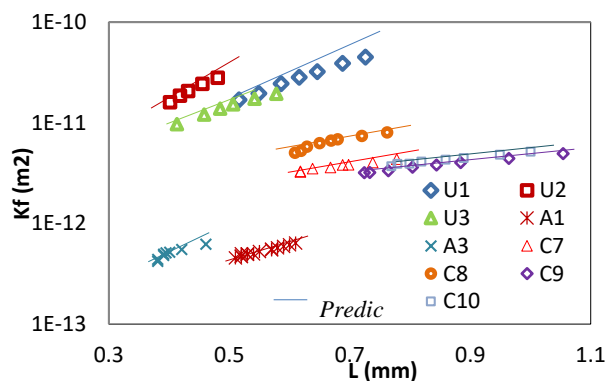
The slope of the prediction line of K_f along L is determined according to Eq.10 on the basis of the fabric geometrical factors, such as R, a and λ. Whereas, the slope itself can reflect the significance of L to K_f. A higher slope indicates a more important effect of L on K_f, which means a slight variation of L would give rise to a larger change of K_f. In this regard, fabrics U_3 and A_3 are the most sensitive fabrics for the effect of L on K_f, as shown in Fig.9. This can be interpreted by the geometrical specifications in Table 1, showing them with clear gaps (yarn spacing subtracted by yarn width) between yarns which cause larger room for accommodating the yarns deformation than the tight overlapping-yarns fabrics, such as fabric A_1 and twill woven fabrics. In Fig.9, fabrics A_1 ($\emptyset$=0) and A_3 ($\emptyset$=0.32%) are much denser fabrics with lower K_f values and greater resistance to air flow than that of twill fabrics C_7 to C_{10} ($\emptyset$>1%) and loose plain fabrics U_1 to U_3 ($\emptyset$>1.5%). It is noted that fabrics C_9 and C_{10} from different finishing process show close K_f values and similar relationships of L and K_f. Moreover, the K_f values of twill woven fabrics (C_x) are in the middle of loose plain fabrics (U_x) and tight plain fabrics (A_x), disclosing the importance of the fabric porosity $\emptyset$ (or (1-$\emptyset$) called fabric cover factor) in K_f prediction. The effect of L on K_f can also be interpreted by Fig.7c, which illustrates the resistance of inter-yarn gaps to air flow from the original and compressed (thick and thin) flow channels. As L increases, the sub-vector of resistance to air flow is decreased in planar (dx) and increased in through-thickness direction (dz). The frictional interaction between air and yarn cross-sectional wall causing hydraulic resistance to air flow becomes smaller with an increase of L. This is also revealed by Eq.1 where L and K_f are in linear proportion under the constant ratio of ΔP to V.

Sensitivity of LPC to K_f

Figure 9 Measured fabric real permeability along transient fabric thickness under LPC
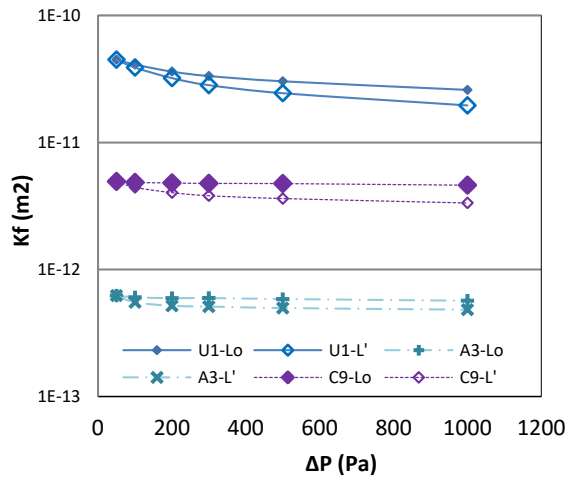
Figure 10 Comparison of the measured K_f with (L') and without (L^o) fabric LPC

Figure 10 shows the relationship of K_f and ΔP values for three selected woven fabric samples, where 'L^o' and 'L'' are initial thickness (constant) and transient thickness (dynamic), respectively. The K_f values were calculated according to Eq.1 based on the two kinds of L values. More than 30% difference of K_f values for a sample under 200 Pa of LPC show the high sensitivity of K_f to LPC. As discussed for Fig.5, LPC reduces L significantly, then 'L^o' is only an ideal value in obtaining K_f. With the increase of air ΔP on both fabric sides, the difference between the 'ideal' and the 'real' K_f values is increasing, as shown more than 50% difference of K_f for each fabric at 1000 Pa in Fig.10. Normally, the K_f value at constant L^o should be constant, such as the horizontal lines of fabrics A_3 and C_9, nonetheless, it is a decline along ΔP for fabric U_1 which may be ascribed to the slight nonlinear relationship of the tested V and ΔP values.

In addition, the most decreased amount of L is found below 200 Pa for the easy compaction of yarn crossover and undulated path, while K_f presents the same reduction ratio at this LPC area, especially near the 100 Pa of abscissa. This suggests that the conventional test standards (BS/EN and ASTM) [5,6] of K_f under ΔP values of 50 Pa and 125 Pa should be performed carefully if considering the transient L at this sensitive LPC to woven fabric.

Conclusions

Fabric through-thickness permeability (TTP) measurement is always performed based on different test standards in different countries and regions for different woven formats and geometrical structures. These standards usually suggest a small flow pressure drop applied to a fabric for measuring a flow velocity. Whereas fabric thickness is measured under another pressure drop based on a thickness test standard. Darcy's law is employed to obtain the fabric TTP according to the tested values. This is normally accepted for a fabric TTP measurement. However, this article found that fabric thickness is sensitive to the through-thickness pressure load experimentally, especially below 200 Pa with an evident reduction of thickness. This conflicts with a few standards for measuring the fabric TTP using a constant fabric thickness.

In this article, nine woven fabrics were employed to study the effect of fabric low- pressure compression (LPC) on TTP, and found that the LPC reduces the fabric thickness significantly at the initial stage. Secondly, other fabric in-planar geometrical factors were investigated and found their variation can be ignored during LPC, indicating that fabric thickness can be regarded as the only factor in determining the variation of fabric TTP at LPC stage. Thirdly, it was found a linear relationship between air pressure drop and air velocity, which indicates a linear dependence of TTP on thickness. This is true with lower resistance of thicker fabric to air flow due to less friction between air flow and fabric. Sensitivity study showed that fabric early compression affects the fabric TTP significantly, giving rise to a lower TTP value compared with the TTP from the initial constant fabric thickness. This implies that the fabric thickness should be the value from the compression test under the same pressure drop in the TTP measurement.

References

1. Carman PC., Permeability of saturated sands, soils and clays, The Journal of Agricultural Science, 29：262-273. (1939)　DOI: 10.1017/S0021859600051789

2. Ishikawa T, Chou TW., Stiffness and strength behaviour of woven fabric composites, Journal of Materials Science, 17: 3211-3220. (1982) DOI: 10.1007/BF01203485

3. Potluri P, Sagar TV., Compaction modelling of textile preforms for composite structures, Composite Structures, 86(1-3): 177-185. (2008) DOI: 10.1016/j.compstruct.2008.03.019

4. Ozgen B, Gong H., Yarn geometry in woven fabrics, Textile Research Journal, 81(7): 738-745. (2011) DOI: 10.1177/0040517510388550

5. BS EN ISO 9237: 1995. Textiles – determination of the permeability of fabrics to air. British Standard, 3–5.

6. ASTM D737 R2012. Standard test method for air permeability of textile fabrics. International Standard, 6-8

7. De Jong S, Snaith JW, Michie NA., A mechanical model for the lateral compression of woven fabrics, Textiles Research Journal, 56: 759-767. (1986) DOI: 10.1177/004051758605601208

8. Hu J, Newton A., Low-load lateral-compression behaviour of woven fabrics, Journal of the Textile Institute, 88(3): 242-254. (1997) DOI: 10.1080/00405009708658548

9. Chen B, Cheng AHD, Chou TW., A nonlinear compaction model for fibrous preforms, Composites: Part A 32: 701-707. (2001) DOI: 10.1016/S1359-835X(00)00148-2

10. Lin H, Sherburn M, Crookston J, Long AC, Clifford MJ, Jones IA., Finite element modelling of fabric compression, Modelling and Simulation in Materials Science and Enginnering, 16(3): 1-16. (2008) DOI: 10.1088/0965-0393/16/3/035010

11. Gebart BR., Permeability of unidirectional reinforcements for RTM, Journal of Composites Materials, 26(8): 1101-1133. (1992) DOI: 10.1177/002199839202600802

12. Cai Z, Berdichevesky AL., An improved self-consistent method for estimating the permeability of a fibre assembly, Polymer Composites, 14(4): 314-323. (1993) DOI: 10.1002/pc.750140407

13. Bruschke MV, Advani SG., Flow of generalized Newtonian fluids across a periodic array of cylinders, Journal of Rheology, 37(3): 479-497. (1993) DOI: org/10.1122/1.550455

14. Westhuizen JV, Plessis JPD., An attempt to quantify fibre bed permeability utilizing the phase average Navier-Stokes equation, Composites: Part A, Applied Science and Manufacturing, 27A: 263-269. (1996) DOI: 10.1016/1359-835X(95)00039-5

15. Advani SG, Bruschke MV, Parnas RS., Resin transfer molding flow phenomena in polymeric composites, In 'Flow and rheology in polymer composites manufacturing', ed. S. G. Advani, Elsevier science B. V, Amsterdam. (1994)

16. Endruweit A, Gommer F, Long AC., Stochastic analysis of fibre volume fraction and permeability in fibre bundles with random filament arrangement, Composites: Part A, Applied Science and Manufacturing, 49, 109-118. (2013) DOI: 10.1016/j.compositesa.2013.02.012

17. Kulichenko AV., Theoretical analysis, calculation, and prediction of the air permeability of textiles, Fibre Chemistry, 37(5): 371-380. (2005) DOI: 10.1007/s10692-006-0011-6

18. Befru R, Okur A., Prediction of the in-plane and through-plane fluid flow behaviour of woven fabrics. Textile Research Journal, 83(7): 700-717. (2013)　DOI: 10.1177/0040517512460300

19. Zupin Z, Hladnik A and Dimitrovski K., Prediction of one-layer woven fabrics air permeability using porosity parameters. Textile Research Journal, 82(2): 117-128. (2012) DOI: 10.1177/0040517511424529

20. Xiao XL, Zeng XS, Long AC, Cliford MJ, Lin H, Saldaeva E., An analytical model for through-thickness permeability of woven fabric, Textile Research Journal, 82(5): 492-501. (2012) DOI: 10.1177/0040517511414979

21. Saldaeva E., Through thickness air permeability and thermal conductivity analysis for textile materials, PhD thesis, The University of Nottingham, (2010) http://ethos.bl.uk/Order Details.do ?uin= uk.bl.ethos.537646

22. Xiao XL., Modeling the structure-permeability relationship for woven fabrics, PhD thesis, The University of Nottingham, (2012)http://etheses.nottingham.ac.uk/2895/

23. Lundstrom TS and Hakanson JM., Measurement of the permeability tensor of compressed fibre beds, Transport in Porous Media, 47: 363–380. (2002) DOI: 10.1023/A:1015511312595

24. TexGen. [cited 23/04/2014]: http://texgen.sourceforge.net/index.php/Main_Page

25. CFX 12.1. [cited 23/04/2014]: http://www.parquecientificomurcia.es/en/web/centro-de-supercomputacion/guia- ansys-cfx

26. Bernard LM., An introduction to hydrodynamics & water waves. Springer, p.84(1976)

27. Sutera SP, Skalak R., The history of Poiseuille's law. Annual Review of Fluid Mechanics, 25: 1–19. (1993) DOI: 10.1146/annurev.fl.25.010193.000245

28. Xiao X, Long A, Zeng X., Through-thickness permeability modelling of woven fabric under out-of-plane deformation, Journal of Materials Science, 49(21), 7563-7574. (2014)   DOI: 10.1007/s10853-014-8465-z

29. Carnaby GA, Pan N., Theory of the compression hysteresis of fibrous assemblies, Textile Research Journal, 59: 275-284. (1989)   DOI: 10.1177/004051758905900505

30. Lomov SV, Verpoest I., Compression of woven reinforcements: a mathematical model. Journal of reinforced plastics and composites, 19: 1329-1350. (2000)   DOI: 10.1106/50RF-DQJ7-9RN3-6CPX

31. Aliouche D, Viallier P., Mechanical and tactile compression of fabrics: influence on handle. Textile Research Journal, 70: 939-944. (2000) DOI: 10.1177/004051750007001101